Hydroquinone-ZnO nano-laminate deposited by molecular-atomic layer deposition

Jie Huang,[1] Antonio T. Lucero,[1] Lanxia Cheng,[1] Hyeon Jun Hwang,[1,2] Min-Woo Ha,[3] and Jiyoung Kim[1,a)]
[1]*Department of Material Science and Engineering, the University of Texas at Dallas, Richardson, Texas 75080, USA*
[2]*School of Material Science and Engineering, Gwangju Institute of Science and Technology, Gwangju 500-712, South Korea*
[3]*Department of Electrical Engineering, Myongji University, Yongin, Gyeonggi-do 449-728, South Korea*

(Received 15 December 2014; accepted 18 March 2015; published online 25 March 2015)

In this study, we have deposited organic-inorganic hybrid semiconducting hydroquinone (HQ)/zinc oxide (ZnO) superlattices using molecular-atomic layer deposition, which enables accurate control of film thickness, excellent uniformity, and sharp interfaces at a low deposition temperature (150 °C). Self-limiting growth of organic layers is observed for the HQ precursor on ZnO surface. Nano-laminates were prepared by varying the number of HQ to ZnO cycles in order to investigate the physical and electrical effects of different HQ to ZnO ratios. It is indicated that the addition of HQ layer results in enhanced mobility and reduced carrier concentration. The highest Hall mobility of approximately 2.3 $cm^2/V{\cdot}s$ and the lowest n-type carrier concentration of approximately $1.0 \times 10^{18}/cm^3$ were achieved with the organic-inorganic superlattice deposited with a ratio of 10 ZnO cycles to 1 HQ cycle. This study offers an approach to tune the electrical transport characteristics of ALD ZnO matrix thin films using an organic dopant. Moreover, with organic embedment, this nano-laminate material may be useful for flexible electronics. © *2015 AIP Publishing LLC*.
[http://dx.doi.org/10.1063/1.4916510]

The development of electronic devices requires accurate control of material composition and feasibility of depositing ultra-uniform thin films. It also demands monolayer-scale accuracy on top of complex surfaces or high aspect-ratio features and enable the creation of functionalities within the film by adjusting the concentration and location of individual component.[1–3] Since atomic layer deposition (ALD) satisfies most of these requirements, it has been widely applied in research and industry.[4–11]

More recently, molecular layer deposition (MLD), a thin film fabrication technique specially designed for organic molecule deposition, has attracted attention due to its capability of depositing organic thin films with monolayer level accuracy and freedom of material selection.[12–15] The principle and process of MLD are similar to that of ALD, which involves sequential, self-limiting surface reactions. Researchers have reported several organic thin films being deposited by MLD.[16–20] Laminate structures, which are constructed with two or more layers one after another, have shown interesting semiconducting properties and present potential applications in thin film transistors (TFTs).[21–23] Organic-inorganic hybrid laminates structure can be created by MLD combined with ALD in the same deposition chamber, which we named as molecular-ALD (MALD). Using this approach, organic-inorganic superlattice can be fabricated in a vapor phase with nanometer-precise control and minimized formation of defects during the growth process, particularly when compared to solution based methods.[24,25]

In this letter, we demonstrate the fabrication and characterization of hydroquinone (HQ)/zinc oxide (ZnO) based organic-inorganic superlattice with various ratios deposited using MALD. The resulting hybrid nano-laminates were characterized by physical and electrical manners. And the deposition and conduction mechanism will be discussed.

Silicon (100) wafers (Silicon Valley Microelectronics) were applied as substrates for physical characterization. For electrical measurements, quartz substrates were used in order to avoid current flow through the substrate. Before deposition, UV and ozone (O_3) cleaning was applied for 5 min to remove potential organic contaminates.

All organic-inorganic nano-laminates were deposited using a D100 (NCD Tech, Korea) at 150 °C unless mentioned otherwise. The flow rate of the N_2 carrier gas was 50 sccm. HQ (Sigma-Aldrich) powder was placed in a stainless steel canister and evaporated at 130 °C. ZnO were deposited using diethyl-zinc (DEZ, Sigma-Aldrich) and deionized water as precursors, which were evaporated at 20 °C and 10 °C, respectively. The schematic of HQ-ZnO hybrid thin film deposition process is depicted in Fig. 1. HQ is introduced on top of ethyl-terminated Zn surface. It is expected that HQ molecules are deposited by an exchange reaction between its –OH functional and the ethyl ligand ($-C_2H_5$) of DEZ precursors, while there is no reaction or polymerization between hydroxyls of HQ molecules during a HQ pulse.[26] The following DEZ would react with the phenol terminated surface. Sequentially, we also deposit various thicknesses of ZnO using DEZ-H_2O to prepare different compositional ratios of HQ in ZnO films. In this letter, the ratio of HQ/ZnO is defined by the number of DEZ-H_2O cycles (shown as ×N cycle in Fig. 1) per HQ pulse, which results in organic-inorganic nano-laminate. One

a)jiyoung.kim@utdallas.edu

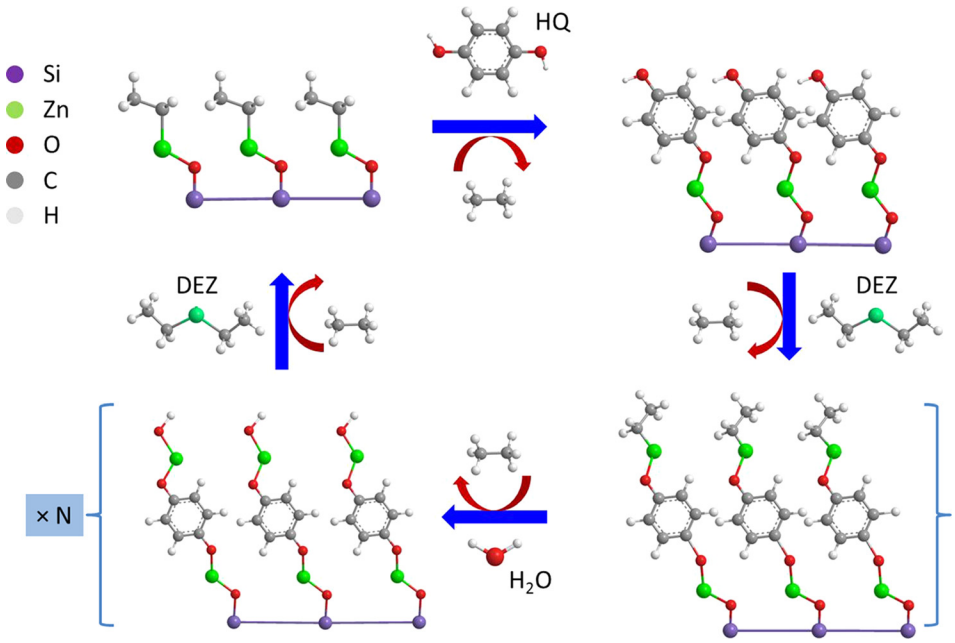

FIG. 1. Schematic mechanism of HQ/ZnO hybrid thin films deposited by MALD. Total MALD cycle consist of HQ-DEZ cycle and ZnO cycle (DEZ-H_2O) to control composition ratio between organic and inorganic layers of nano-laminate.

HQ-DEZ cycle consisted of 1 s exposure of DEZ, 20 s N_2 purge, 10 s exposure of HQ, and 60 s N_2 purge. One ALD cycle consisted of 1 s exposure of DEZ, 20 s N_2 purge, 0.5 s exposure of H_2O, and 20 s N_2 purge.

A spectroscopic ellipsometer (Sentech 800) was used to measure the MALD nano-laminate thickness. A spectral range of 400–850 nm with an incident angle of 75° was set up for measurement. Surface morphology was obtained using an atomic force microscope (AFM, Veeco Model 3100 Dimension V). Silicon cantilevers with a resonance frequency around 289–331 kHz and spring constant about 20–80 N/m were used to scan the sample using tapping mode. X-ray diffraction (XRD) was applied to determine the crystal structure of nano-laminates. The XRD (Rigaku Ultima III) analysis was performed on films deposited on SiO_2/Si substrates with Cu Kα radiation at $\lambda = 1.54$ Å. Cross-sectional transmission electron microscopy (TEM) samples were prepared by lift-out method using a focused ion beam (FIB, FEI Nova 2000) system equipped with a nano-manipulator. All samples were characterized using a field emission TEM (JOEL 2100).

For electrical properties, Hall-effect measurements (LakeShore, 8400 Series) were performed for MALD films. All nano-laminate samples consist of 100 cycles of DEZ/H_2O, with various numbers of HQ/DEZ cycle embedment. Aluminum (Al) contacts were deposited using e-beam evaporation on four corners of 1 cm × 1 cm square samples in a Van der Pauw configuration. The carrier type, carrier concentration, and Hall mobility were all deduced from Hall measurement in magnetic field of 1.7 T at room temperature.[27]

The self-limiting nature of the surface reaction was examined by observing the thickness of HQ/ZnO (1:1) hybrid films deposited for 100 cycles versus HQ dosing time, as shown in Fig. 2(a). The results demonstrate that the HQ reaction on top of –Zn-C_2H_5 is self-limiting and reaches saturation after 10 s of HQ dosage. This implies a self-limiting surface reaction which is analogous to the deposition mechanism in ALD. If we assume the HQ/ZnO (1:1) hybrid thin film is homogenous, that is, all the interfaces inside the hybrid system are ignored for simplicity, the Cauchy model is valid for the fitting of thickness and refractive index. The refractive index of resulting films was as low as approximately 1.7 due to the incorporation of an organic component,[28] i.e., HQ molecules, compared to pure ZnO which has refractive index value of approximately 2.0. The dependence on the number of cycles of HQ/ZnO (1:1) hybrid thin film versus thickness is plotted in Fig. 2(b).

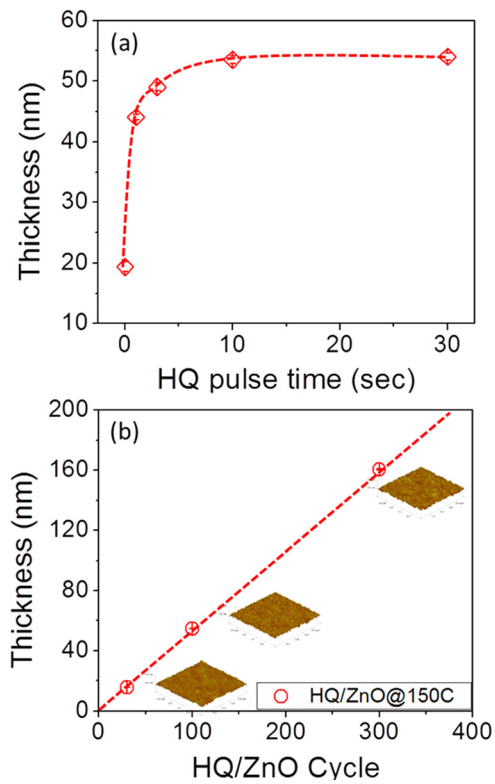

FIG. 2. (a) HQ pulse saturation curve (all thickness was measured after 100 cycles), and (b) growth rate confirmation of HQ/ZnO (1:1) hybrid thin films deposited at 150 °C (Insets are surface morphology images of relevant films characterized by AFM tapping mode).

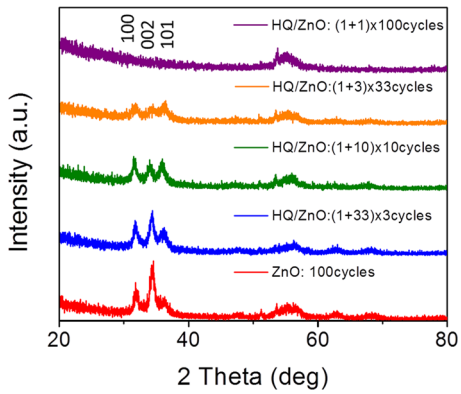

FIG. 3. XRD patterns of HQ/ZnO nano-laminates deposited at 150 °C on silicon substrates.

The measured growth rate is approximately 5.4 Å/cycle, where a cycle consists of DEZ-HQ-DEZ-H_2O exposure. The growth rate is quite reasonable considering the size of a benzene ring (approx. 3.6 Å) plus one molecule of ZnO (approx. 2.0 Å),[29] indicating the HQ molecules are more likely chemisorbed perpendicular to the sample surface. Surface morphology was studied by AFM, as shown in the inset of Fig. 2(b). The HQ/ZnO (1:1) deposited at 150 °C for 30 cycles has a relatively low RMS roughness value of 0.288 nm, compared to the roughness of Si substrate (approx. 0.3 nm). After 100 and 300 cycles, the roughness is nearly constant (RMS of 0.351 nm and 0.378 nm, respectively). Overall, the surface roughness does not strongly depend on film thickness and is very smooth even after hundreds of cycles of deposition.

Effects of HQ/ZnO ratio on physical and electrical characteristics of hybrid system have been investigated. All HQ/ZnO nano-laminates were deposited with the equivalent number of DEZ/H_2O cycles, i.e., 100. Pure ZnO was deposited for 100 cycles at the same temperature using the MALD system as a reference for both physical and electrical characterization. XRD patterns of the nano-laminates are shown in Fig. 3. All of the diffraction peaks can be indexed according to the wurtzite structure of ZnO.[30,31] The data clearly illustrate that by increasing the HQ component, the laminate becomes more amorphous in crystal structure. The HQ/ZnO film with 1:1 ratio is almost completely amorphous, with only a weak sign of ZnO wurtzite structure observed in the XRD pattern, indicating the blocking effect of HQ on ZnO crystal growth. Direct observation of the nano-laminate structure was performed by cross-sectional TEM, as shown in Fig. 4. As expected, these images, along with the contrast difference of these nano-laminates shown as insets, indicated that nano-laminates have a layer-by-layer structure consisting of a ZnO matrix and uniform HQ in-between layers rather than island growth. Bright lines are clearly visible among the dark ZnO matrix, whereas there is no line in the ZnO reference sample. Since both carbon and hydrogen are lighter elements than zinc, it is expected that those bright lines correspond to HQ layers. These results provide direct evidence of the superlattice structure.

For electrical properties, Hall measurements were performed to extract the mobility and carrier concentration from a pure ZnO thin film (reference sample) as well as HQ/ZnO ratios of 1:100, 1:33, and 1:10 nano-laminates, as summarized in Fig. 5. All samples are n-type semiconductors. By introducing a single layer of HQ between ZnO and the substrate, the mobility increased more than 50% (from approx. 1.0 $cm^2/V{\cdot}s$ to 1.6 $cm^2/V{\cdot}s$), whereas the carrier concentration dropped from approx. $6.5 \times 10^{18}/cm^3$ to $5.0 \times 10^{18}/cm^3$. The mobility of the HQ/ZnO (1:33) laminate (approx. 2.2 $cm^2/V{\cdot}s$) is more than double of pure ZnO. The mobility of the HQ/ZnO (1:10) laminate (approx. 2.3 $cm^2/V{\cdot}s$) did not increase significantly relative to the HQ/ZnO (1:33) sample, as shown in Fig. 5(a). We obtain mobility of HQ/ZnO nano-laminates, which results from HQ ratio without consideration of crystallinity effects.[32] Further investigation regarding

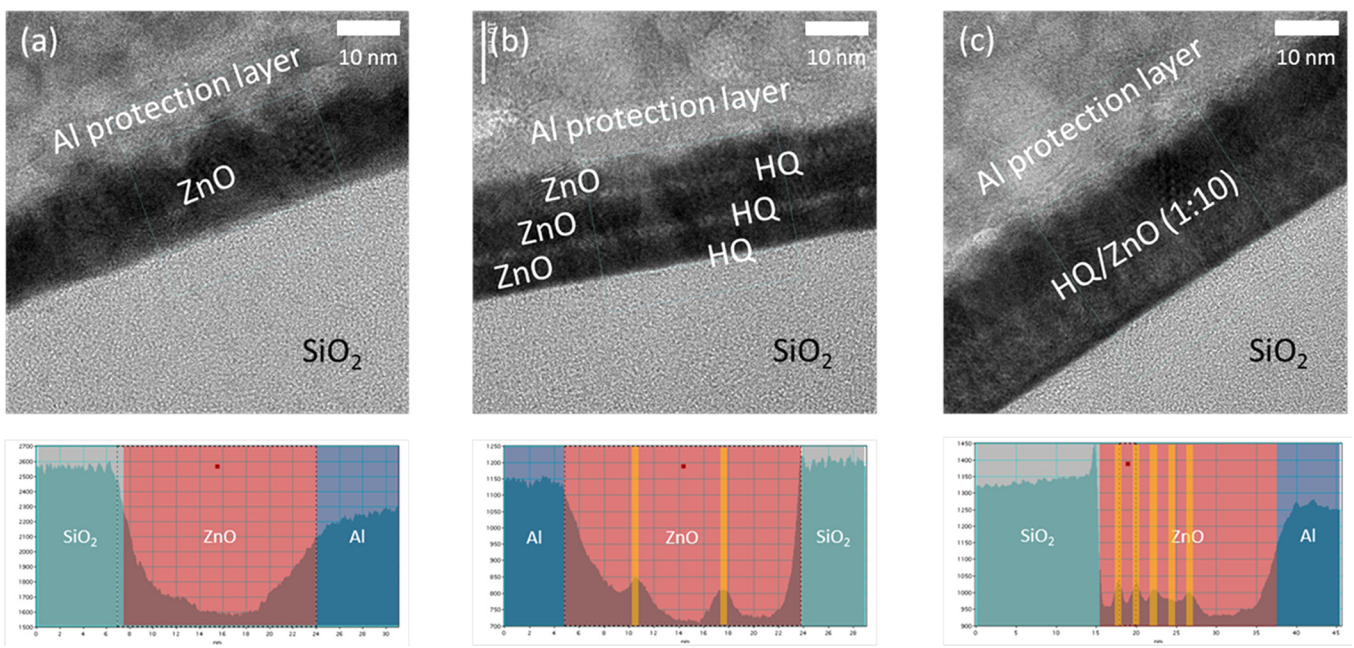

FIG. 4. Cross-sectional TEM images of (a) ZnO, (b) HQ/ZnO (1:33), and (c) HQ/ZnO (1:10) nano-laminates. The insets are the contrast profiles of ZnO thin film and HQ/ZnO nano-laminates for the corresponding TEM images.

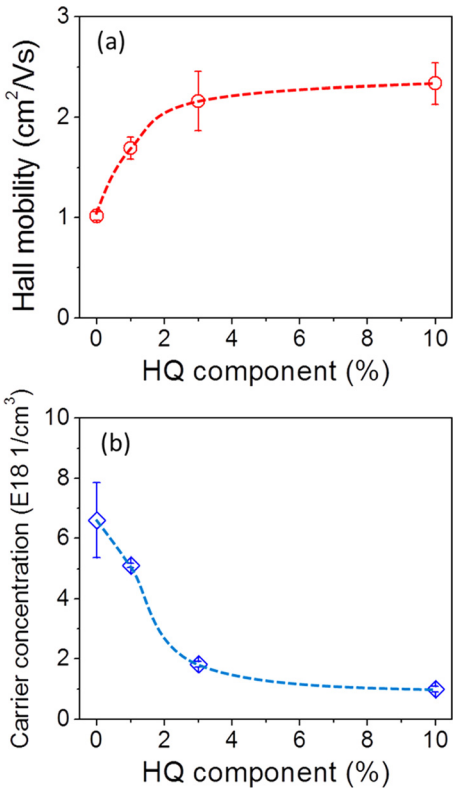

FIG. 5. (a) Hall mobility and (b) carrier concentration of HQ/ZnO nano-laminates as a function of HQ component.

crystallinity effects on electrical transport characteristics will be performed. On the other hand, the carrier concentration of HQ/ZnO nano-laminates dropped from approximately $6.5 \times 10^{18}/\text{cm}^3$ for pure ZnO to approximately $1.8 \times 10^{18}/\text{cm}^3$ for the HQ/ZnO (1:33) sample, and further decreased to approximately $1.0 \times 10^{18}/\text{cm}^3$ for the HQ/ZnO (1:10) sample, as shown in Fig. 5(b).

This result is promising because RF magnetron sputtering is the dominant method for ZnO semi-conductive thin film deposition,[33,34] whereas, in general, ALD-deposited ZnO thin films are too conductive for TFT applications due to the high carrier concentration with typical value of approximately $10^{19}\,\text{cm}^{-3}$ (normally, for TFT applications, carrier concentration should be lower than $10^{18}\,\text{cm}^{-3}$).[35] Non-stoichiometry due to oxygen vacancies (V_o) and/or zinc interstitials (Zn_i) is generally thought to be responsible for the high conductivity in ALD-deposited ZnO.[30,36,37] In most doped ZnO thin film studies, in which dopants such as Al served as n-type donors,[29,38,39] carrier density can be increased due to the generation of V_o or Zn_i, and the mobility are normally decreased, possibly because of impurity scattering. In contrary, it is relatively difficult to obtain p-type doping in wide-band-gap semiconductors, including ZnO, possibly because dopants may be compensated by low-energy native defects, such as Zn_i or V_o, or low solubility of the dopant in the host material.[40–42] In the HQ/ZnO system, the higher the HQ to ZnO ratio, the higher mobility and the lower carrier concentration was observed. It is possible that our HQ embedment involves defect-related mechanism to reduce electrons, i.e., hydroxyl groups decrease oxygen vacancies as well as electron concentration. It is also possible that HQ may serve as a p-type dopant for the hybrid system. Further study is required to elucidate a mechanism of the doping effects of HQ. For mobility improvement, unlike conventional crystallinity effect, i.e., the higher the crystallinity, the higher the carrier mobility, the inverse relationship between the mobility and crystallinity of our hybrid system may be attributed to the introduction of HQ layers caused reduction of scattering events. By adjusting the HQ/ZnO ratio for the nano-laminates, we can alter the electrical properties of the thin films. This study offers an approach to tune the electrical transport characteristics of ALD ZnO matrix thin films using organic dopants. Moreover, limited publications have been reported using organic p-dopants in semiconductors.[43,44] Mainly because it is still a challenge to quantitatively describe the doping process in organic systems, let alone the *in-situ* layer-by-layer doping. From our results, introducing organic dopants, even layer so, potentially it offers an opportunity for HQ-ZnO films to be used for flexible electronics.

In summary, we investigated the growth characteristics of HQ/ZnO organic-inorganic hybrid thin films. Using MALD technique, we design a deposition scheme of HQ/ZnO nano-laminates with a variety of HQ to ZnO ratios. The physical properties of organic-inorganic superlattice thin films are investigated by ellipsometry, AFM, XRD, and cross-sectional TEM, indicating a well-controlled self-limiting layer-by-layer growth. Hall-effect measurements demonstrate that the addition of HQ has a significant impact on the electrical characteristics of ZnO matrix film by improving the mobility and reducing the carrier concentration. The highest Hall mobility of approx. $2.3\,\text{cm}^2/\text{V}\cdot\text{s}$ and the lowest carrier concentration of approx. $1.0 \times 10^{18}/\text{cm}^3$ were achieved with the HQ/ZnO (1:10) sample. Using this approach, organic component HQ are embedded into inorganic ZnO thin films to form hybrid nano-laminates, which can be applied as semiconducting material for future electronics applications.

This research was financially supported by Kookmin University (through UTD-KMU In-FUSION program), Texas Research Incentive Program (TRIP), and MKE-COSAR-KETI through Korea-U.S. collaboration R/D program.

[1]J. Wen and G. L. Wilkes, Chem. Mater. **8**, 1667 (1996).
[2]S. W. Pyo, D. H. Lee, J. R. Koo, J. H. Kim, J. H. Shin, and Y. K. Kim, Jpn. J. Appl. Phys., Part 1 **44**, 652 (2005).
[3]W. E. Tenhaeff and K. K. Gleason, Adv. Funct. Mater. **18**, 979 (2008).
[4]J. W. Elam, Z. A. Sechrist, and S. M. George, Thin Solid Films **414**, 43 (2002).
[5]C. Bae, H. Yoo, S. Kim, K. Lee, J. Kim, M. M. Sung, and H. Shin, Chem. Mater. **20**, 756 (2008).
[6]J. Kim and T. Kim, JOM **61**, 17 (2009).
[7]J. Huang, M. Lee, and J. Kim, J. Vac. Sci. Technol. A **30**(1), 01A128 (2012).
[8]P. Sivasubramani, T. J. Park, B. E. Coss, A. Lucero, J. Huang, B. Brennan, Y. Cao, D. Jena, H. Xing, R. M. Wallace, and J. Kim, Phys. Status Solidi (RRL) **6**, 22 (2012).
[9]Y. J. Suh, N. Lu, S. Y. Park, T. H. Lee, S. H. Lee, D. K. Cha, M. G. Lee, J. Huang, S. Kim, B. Sohn, G. Kim, M. J. Ko, J. Kim, and M. J. Kim, Micron **46**, 35 (2013).
[10]L. Cheng, X. Qin, A. Lucero, A. Azcatl, J. Huang, R. M. Wallace, K. Cho, and J. Kim, ACS Appl. Mater. Interfaces **6**(15), 11834 (2014).
[11]J. Huang, M. Lee, A. Lucero, L. Cheng, and J. Kim, J. Phys. Chem. C **118**(40), 23306 (2014).

[12]S. M. George, B. Yoon, and A. A. Dameron, Acc. Chem. Res. **42**(4), 498 (2009).
[13]B. Yoon, D. Seghete, A. S. Cavanagh, and S. M. George, Chem. Mater. **21**, 5365 (2009).
[14]Q. Peng, B. Cong, R. M. VanGundy, and G. N. Parsons, Chem. Mater. **21**, 820 (2009).
[15]P. W. Loscutoff, H. Zhou, S. B. Clendenning, and S. F. Bent, ACS Nano. **4**(1), 331 (2010).
[16]S. Cho, G. Han, K. Kim, and M. M. Sung, Angew. Chem., Int. Ed. **50**, 2742 (2011).
[17]H. Zhou and S. F. Bent, ACS Appl. Mater. Interfaces **3**, 505 (2011).
[18]A. I. Abdulagatov, R. A. Hall, J. L. Sutherland, B. H. Lee, A. S. Cavanagh, and S. M. George, Chem. Mater. **24**, 2854 (2012).
[19]B. H. Lee, B. Yoon, V. R. Anderson, and S. M. George, J. Phys. Chem. C **116**, 3250 (2012).
[20]J. Huang, M. Lee, A. Lucero, and J. Kim, Chem. Vap. Deposition **19**, 142 (2013).
[21]C. R. Kagan, D. B. Mitzi, and C. D. Dimitrakopoulos, Science **286**, 945 (1999).
[22]B. Fluegel, Y. Zhang, A. Mascarenhas, X. Huang, and J. Li, Phys. Rev. B **70**, 205308 (2004).
[23]Y. Zhang, G. M. Dalpian, B. Fluegel, S. H. Wei, A. Mascarenhas, X. Y. Huang, J. Li, and L. W. Wang, Phys. Rev. Lett. **96**, 026405 (2006).
[24]P. Sundberg, A. Sood, X. Liu, L. Johansson, and M. Karppinen, Dalton Trans. **41**, 10731 (2012).
[25]P. Sundberg, A. Sood, X. Liu, and M. Karppinen, Dalton Trans. **42**, 15043 (2013).
[26]B. Yoon, B. H. Lee, and S. M. George, J. Phys. Chem. C **116**, 24784 (2012).
[27]M. I. Medina-Montes, S. H. Lee, M. Perez, L. A. Baldenegro-Perez, M. A. Quevedo-Lopez, B. Gnade, and R. Ramirez-Bon, J. Electron. Mater. **40**(6), 1461 (2011).
[28]B. H. Lee, B. Yoon, A. I. Abdulagatov, R. A. Hall, and S. M. George, Adv. Funct. Mater. **23**, 532 (2013).
[29]B. Shong, K. T. Wong, and S. F. Bent, J. Phys. Chem. C **116**, 4705 (2012).
[30]U. Ozgur, Y. I. Alivov, C. Liu, A. Teke, M. A. Reshchikov, S. Dogan, V. Avrutin, S. Cho, and H. Morkoc, J. Appl. Phys. **98**, 041301 (2005).
[31]T. Tynell, H. Yamauchi, M. Karppinen, R. Okazaki, and I. Terasaki, J. Vac. Sci. Technol. A **31**(1), 01A109 (2013).
[32]K. Ellmer and R. Mientus, Thin Solid Films **516**, 4620 (2008).
[33]D. K. Kim and H. B. Kim, J. Alloys Compd. **509**, 421 (2011).
[34]S. H. Jeong, J. W. Lee, S. B. Lee, and J. H. Boo, Thin Solid Films **435**, 78 (2003).
[35]S. K. Kim, C. H. Hwang, S. H. Ko Park, and S. J. Yun, Thin Solid Films **478**, 103 (2005).
[36]G. Neumann, Phys. Status Solidi B **105**, 605 (1981).
[37]A. Janotti and C. G. Van de Walle, Rep. Prog. Phys. **72**, 126501 (2009).
[38]N. P. Dasgupta, S. Neubert, W. Lee, O. Trejo, J. Lee, and F. B. Prinz, Chem. Mater. **22**, 4769 (2010).
[39]D. Lee, H. Kim, J. Kwon, H. Choi, S. Kim, and K. Kim, Adv. Funct. Mater. **21**, 448 (2011).
[40]C. G. Van de Walle, D. B. Laks, G. F. Neumark, and S. T. Pantelides, Phys. Rev. B **47**, 9425 (1993).
[41]W. Walukiewicz, Phys. Rev. B **50**, 5221 (1994).
[42]T. Tsukazaki, A. Ohtomo, T. Onuma, M. Ohtani, T. Makino, M. Sumiya, K. Ohtani, S. F. Chichibu, S. Fuke, Y. Segawa, H. Ohno, H. Koinuma, and M. Kawasaki, Nat. Mater. **4**, 42 (2004).
[43]S. Olthof, W. Tress, R. Meerheim, B. Lüssem, and K. Leo, J. Appl. Phys. **106**, 103711 (2009).
[44]J. Lee, H. Kim, K. Kim, R. Kabe, P. Anzenbacher, Jr., and J. Kim, Appl. Phys. Lett. **98**, 173303 (2011).

2015-3

Hydroquinone-ZnO Nano-Laminate Deposited by Molecular-Atomic Layer Deposition

UTD AUTHOR(S): Jie Huang, Antonio T. Lucero, Lanxia Cheng, Hyeon Jun Hwang, Jiyoung Kim

Huang, J., A. T. Lucero, L. Cheng, H. J. Hwang, et al. 2015. "Hydroquinone-ZnO nano-laminate deposited by molecular-atomic layer deposition." Applied Physics Letters 106(12): doi:10.1063/1.4916510.